Journal of Medical Phyto Research
Vol. 2, Article 2, (14-26)

ISSN: 2577-6541
Doi: 10.31013/2001f

Higher bioactivity cannabidiol in greater concentration more greatly reduces valvular interstitial cell calcification

D. Cushing[1]*, D. Goakar[2], & B. Joseph[1,2]

[1]: Peak Health Center, Los Gatos, CA

[2]: ImmunAG LLP, Goa, India

*For inquiries, email corresponding author at donish@peakhealth.center

Abstract:

Valvular interstitial cells (VICs) are integral to heart valve homeostasis and structural leaflet integrity. Aberrant calcification of VICs leads to dangerous diseases including calcific aortic valve disease. VIC calcification can be reduced through modulation of the MAPK/ERK cascade by selective antagonism of the CB2 receptor. This is a well-studied target of Cannabidiol (CBD). Recently, it has become increasingly understood that not all CBD samples have the same degree of bioactive potential (bioactivity). The present study seeks to determine whether levels of CBD bioactivity have different effects on VIC calcification reduction. VICs were isolated from porcine aortic valve leaflets, induced to calcify, and treated with CBD or left untreated. CBD of varying bioactivity was clustered into 8 different levels (.20, .30, .50, .60, .70, .80, .90, and .95.) by rounding. Concentrations of 5, 10, 25, 40, and 100 mg were examined. Means, standard deviations, minimum, and maximum calcification reduction values for each combination of bioactivity and mg concentration are provided. Two 1x5 repeated measures ANOVAs on mg concentrations, holding bioactivity at .20, and at .95 , respectively, were performed. A 2x2 robust mixed ANOVA confirmed an interaction between bioactivity and mg concentration (*psihat* = -36.5, $p < .001$). Calcification was most reduced by the .95 bioactivity, 100 mg concentration treatment ($M = 55\%$, $SD = 6.66\%$). These results indicate that bioactivity is of central importance when considering CBD as a treatment for VIC calcification reduction.

The valves of the human heart are supple, flow-regulating membranes within a complex multichambered pump (Mohler et al., 2001; Butcher, Simmons, & Warnock, 2008). Within these valves, among an extracellular matrix, exist valvular interstitial cells (VICs), which are integral to heart valve homeostasis and structural leaflet integrity (Hjortnaes et al., 2015; Taylor, Batten, Brand, Thomas, & Yacoub, 2003). Calcification of VICs causes disruption of interstitial cell mechanical phenotype, and drives disorganization of the interstitial matrix, nodule formation, and pro-calcific signaling (Farrar, Pramil, Richards, Mosher, & Butcher, 2016). This can lead to any number of dystrophic calcification diseases of the heart, which each can increase the risk for developing other cardiovascular diseases (e.g., valvular stenosis, see Michel & Dipchand, 2017; de Simone et al., 2010; Gerdts et al., 2015).

Novel therapeutic targets for cardiovascular calcification reduction include cannabinoid receptor 2 (CB2; Kaschina, 2016). CB_2 is present in osteoclasts, osteoblasts, and osteocytes (Ofek et al., 2006; Idris, Sophocleous, Landao-Bassonga, van't Hof, & Ralston, 2008; Idris et al., 2005). CB_2 is upregulated in calcifying heart valves (Naito et al., 2010). CB_2 agonists, such as anandamide, have been shown to stimulate extracellular signal-regulated kinase (ERK) activation (McAllister & Glass, 2002). Greater ERK activation yields greater calcific nodule formation in VICs (Gu & Masters, 2009). Thus, antagonism or inverse agonism of CB_2 should yield reductions in calcification.

Cannabidiol (CBD), the major nonpsychotropic component found in *Cannabis Sativa* (Ligresti Petrocellis, & Di Marzo, 2016) and recently, in a non-cannabis source (Kriya Brand Humulus; see Cushing, Kristipati, Shastri &

Concentration (mg)	Measure	Bioactivity							
		.20	**.30**	**.50**	**.60**	**.70**	**.80**	**.90**	**.95**
5	*M*	5.17	6.16	7.63	7.99	10.06	14.32	18.06	19.42
	SD	0.83	0.54	0.88	0.85	1.28	1.35	1.22	1.8
	Min	3.8	5.2	5.3	6.2	7.3	11.3	14.6	15.4
	Max	6.9	7.3	9.1	10.4	13.6	16.6	21	22.1
10	*M*	4.95	6.24	9.77	11.8	14.33	20.03	25.04	25.56
	SD	0.62	0.66	0.99	1.1	1.48	2.5	2.62	3.04
	Min	3.7	4.9	7.7	9.2	10.2	15.9	20.5	18.5
	Max	6.2	7.5	11.7	14.3	17.2	24.6	30.3	32.5
25	*M*	6.07	6.23	10.89	13.75	16.55	24.94	30.51	32.69
	SD	0.54	0.89	0.8	0.95	1.34	2.63	3.02	4.33
	Min	4.8	4.6	9.5	10.5	14.3	20.2	23.5	26.3
	Max	7.1	8.1	12.5	15.3	18.6	30.3	35.6	42.6
40	*M*	5.19	7.13	14.2	19.23	24.7	28.54	40.09	42.98
	SD	0.75	0.76	1.4	1.5	3.2	3.02	2.77	4.8
	Min	3.6	5.1	12	168	18.9	22.4	33.7	35.8
	Max	6.9	8.1	17.1	21.9	33	34.6	44.6	54.5
100	*M*	6.1	7.2	16.1	21.54	30.71	37.74	48.52	55
	SD	0.58	0.64	1.05	1.22	2.18	2.87	4.27	6.66
	Min	5.2	6	14.1	18.3	25.8	31.7	37.6	41.9
	Max	7.5	8.4	18.1	23.7	35.6	44.4	54.7	66.1

Table 1: Calcification reduction by CBD mg concentration and bioactivity. All calcification reductions are presented as percentages.

Joseph, 2018). CBD acts as an inverse agonist or antagonist at CB_2 (Thomas, Baillie, Phillips, Razdan, Ross, & Pertwee, 2007). CBD suppresses osteoclast formation but stimujlates osteoclast functioning through antagonism of G-coupled protein receptor 55 (GPR55; Whyte et al., 2009)[1].

The present study examines the effect that CBD samples of varying bioactivities (See Cushing, Kristipati, Shastri, & Joseph, 2018) and varying mg concentrations have on the calcification of porcine VICs in vitro. If VIC samples treated with CBD calcify less, this would implicate CBD as a potential prophylactic treatment for valvular calcification diseases. If CBD bioactivity impacts the magnitude of calcification reduction, this would re-emphasize the importance of verifying bioactivity levels prior to scientific experimentation. If higher bioactivity CBD corresponds to greater reductions in calcification, this would suggest that higher bioactivity CBD should be preferred by medical professionals.

Results:

Multiplate wells containing calcifying VICs from 27 different tissue samples were treated with CBD of 8 different bioactivities, and 5 different mg concentrations, or left untreated. Average calcification was computed using the number of nodules per well, and the average area per nodule. Average total nodule area for untreated wells was 3.27 mm^2 (*SD* = 0.32, *min* = 0.5, *max* = 4.0) per well. All reported percent reductions in calcification were computed by dividing average nodule area of treated wells from 3.27 mm^2. CBD samples were clustered according to their bioactivity levels around the values, .20, .30, .50, .60, .70, .80, .90, and .95. Mg dosages of 5, 10, 25, 40, and 100 were examined.

[1] It bears noting that valve calcification often occurs in tandem with inflammation. CBD has anti-inflammatory that likely owe to the dynamic regulation of multiple activity-dependent pathways, including TRPV1, TRPV2, and TRPA1 (Petrocellis et al., 2011; Qin et al., 2008; Bisogno et al., 2001; Costa et al., 2004), 5HT1α receptors (Pazos et al., 2013), glycine receptors (Ahrens et al., 2009), TRPM8 channels (De Petrocellis et al., 2011), T-type voltage-gated calcium channels (Ross, Napier, & Connor, 2008), G protein-coupled receptor GPR55 (Ross, 2009), and several others (For a comprehensive review, see French et al., 2017). These pathways may also directly, or indirectly, influence calcification (e.g., Whyte et al., 2009). CB_2 transduces many immunomodulatory and anti-inflammatory effects as well (Mukhopadhyay et al., 2010; Steffens et al., 2005).

Reduction in Calcification of VIC cells: Comparing bioactivites across concentrations

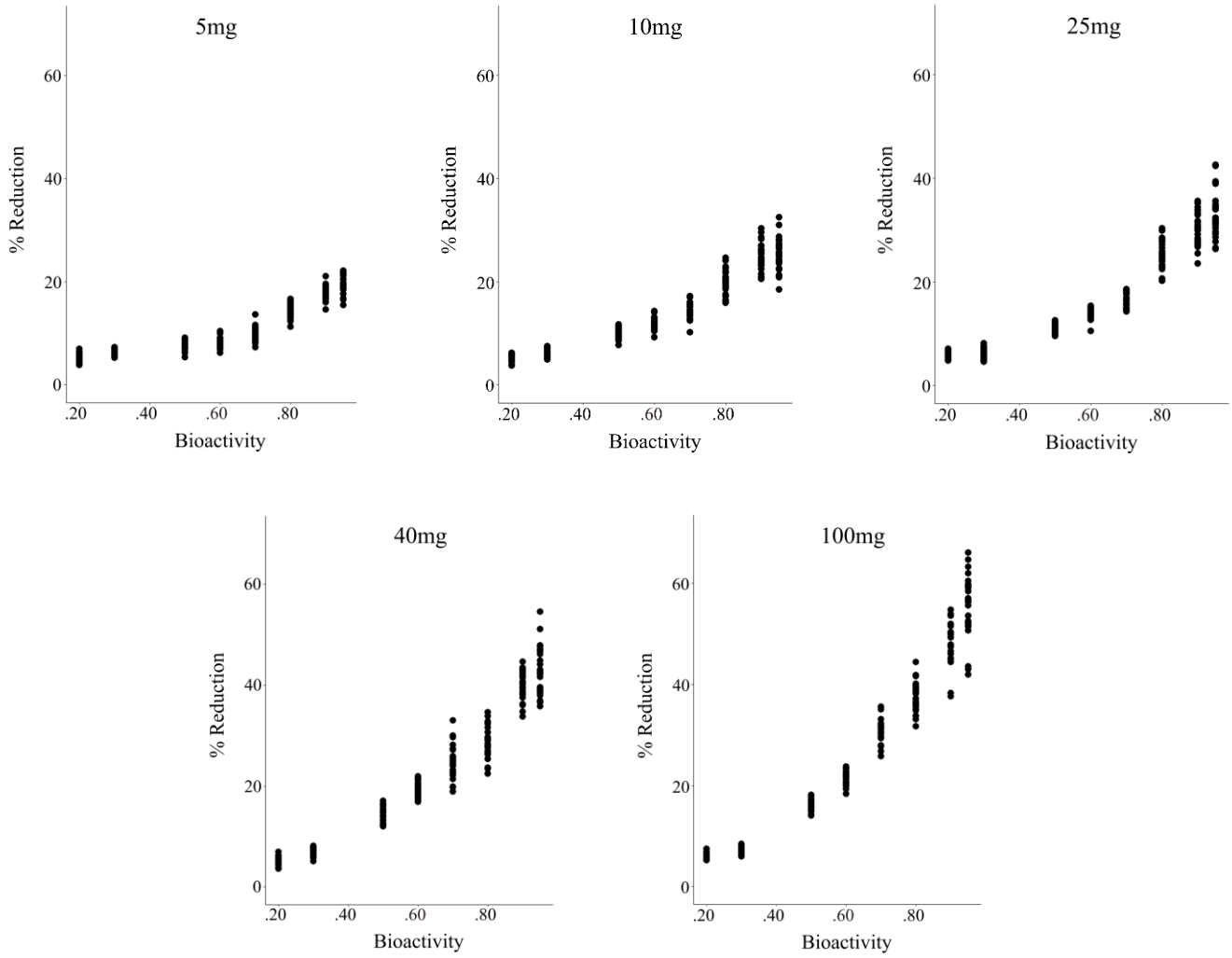

Figure 1: Across all five mg concentrations, there was greater calcification reduction amidst exposure to higher bioactivity CBD. Variance increased as reduction proportions came closer to .5.

Exploratory Data Analysis

Means, standard deviations, and minimum and maximum values for every tested bioactivity level at every tested mg concentration are provided in Table 1. (All data are provided in Appendix.) Higher bioactivities and higher concentrations each corresponded with reductions in calcification. At all five concentrations, with increases in bioactivity, calcification appeared to reduce exponentially (See Figure 1). Variance between the calcification reductions of each sample also increased as bioactivity increased. For example, the group with the highest reduction values (100 mg, .95 bioactivity) showed between 40% and 67% reduction (M = 55%). This group also had the greatest standard deviation (SD = 6.66%). Despite increased variability at higher reduction scores, meaningful differences appeared to exist between bioactivity levels. For example, for every mg concentration, the minimum calcification reduction elicited by .95 bioactivity CBD was still greater than the maximum calcification reduction elicited by .70 bioactivity CBD.

Comparing Low bioactivity CBD across mg concentrations

A 1x5 repeated measures ANOVA was conducted to examine whether differences existed between the various mg concentrations (5, 10, 25, 40, 100) among VIC samples treated with .20 bioactivity CBD (See Figure 2). Mauchley's Test found no violation to the assumption of

Reduction in Calcification of VIC cells: Comparing low and high concentrations across low and high bioactivities

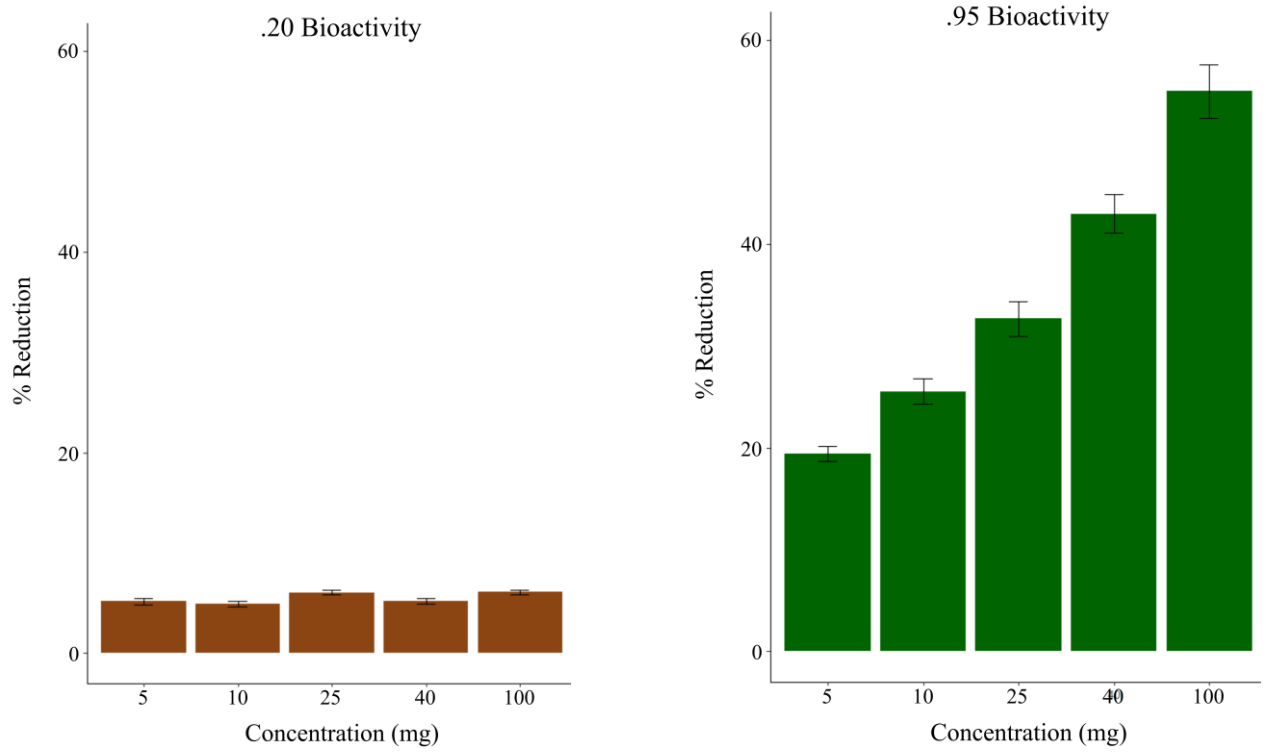

Figure 2: When bioactivity was very low, concentration made a negligible, inconsistent difference. When bioactivity was very high, higher concentrations yeilded greater calcification reductions.

sphericity between samples, $W = .759$, $p = .667$. The RM ANOVA found a significant difference among dosages on VIC calcification reduction within the .20 Bioactivity test group, $F(4, 104) = 18.90$, $p < .001$, $\eta^2_G = .354$. Post-hoc comparisons using the Bonferroni correction indicated that test samples exposed to dosages of 25 mg and 100 mg showed more reduction in VIC calcification than dosages 5, 10, and 40 mg. In all significant post-hoc comparisons, $p < .001$. The differences between these means were small (all $M_{diff} < 1.15\%$).

Comparing high bioactivity CBD across mg concentrations

A 1x5 repeated measures ANOVA was conducted to examine whether differences existed between the various mg concentrations among VIC samples treated with .95 bioactivity CBD (See Figure 2). Mauchley's Test found a possible violation to the assumption of sphericity, $W = .331$, $p = .0014$. A repeated measures ANOVA with a Greenhouse-Geisser correction found a significant difference among dosages on VIC calcification within the .95 bioactivity test group, $F(4, 104) = 260.13$, $p < .001$ $\eta^2_G = .894$. Post-hoc comparisons using the Bonferroni adjustment indicated significant differences across every group. In all significant post hoc comparisons, $p < .0000001$. The differences between these means were much larger (largest $M_{diff} = 35.58\%$).

Examining the interaction between bioactivity and concentration

Since there was an obvious trend across the data showing that higher bioactivity and concentration each lead to greater reductions in calcification, a 2x2 mixed ANOVA was attempted to better understand the degree to which bioactivity and dosage interact. Since the increase in calcification reduction appeared to occur similarly across all mg concentrations, we simplified our statistical approach by examining only the lowest and highest bioactivities and concentrations.

Levene's test showed heterogeneous variances, $W = 23.42$, $p < .001$. Arcsine transformation was unable to

render the variances homogeneous, $W = 16.04$, $p < .001$. Thus, a Robust 2x2 ANOVA using a median estimator was conducted on the original values. It found significant effects of bioactivity as a main effect (*psihat* = 64.7, $p < 0.001$), of concentration as a main effect (*psihat* = -37.5, $p < .001$), and of an interaction between bioactivity and concentration (*psihat* = -36.5, $p < .001$).

Conclusions

At high bioactivities and concentrations, calcification was reduced greatly. At lower bioactivities, mg concentration played an inconsistent role in calcification reduction. At high bioactivities, calcification reduction increased significantly at higher concentrations. A significant interaction effect was found between bioactivity and concentration through a robust estimation technique. Taken together, these results suggest that the bioactivity of the CBD is of central importance when considering the efficacy of CBD as a VIC calcification treatment.

Discussion:

In this study, CBD was shown to be effective at reducing porcine VIC calcification in vitro, with the highest bioactivity CBD at the highest concentration showing the greatest reductions ($M = 55\%$).

Within this experiment, we find ERK inhibition the most likely mechanism by which CBD chiefly reduced VIC calcification (see Gu & Masters, 2009). If this judgment is correct, then the differential calcification reduction caused by bioactivity level implies the differential inhibition of ERK activity. The implications of this are vast.

The ERK pathway links diverse extracellular stimuli to proliferation, differentiation, survival, and vascularization (Roy et al, 2001, Salasznyk et al, 2004; Lewis, Shapiro & Ahn, 1998; Depeille, 2007). A tremendous number of diseases can be affected through its modulation, including cancers (e.g., Wagner & Nebreda, 2009; Huang et al., 2008; Herrera, Carracedo, Diez-Zaera, Guzmán, & Velasco, 2005; Milella et al., 2001). For example, in conjunction with radiation, the MAPK p38 pathway was one of the main drivers of CBD-induced cell death in Glioblastoma (Ivanov et al., 2017). Additionally, the modulation by CBD of ERK and ROS pathways lead to the down-regulation of Id-1 expression and the up-regulation of Id-2, thereby inhibiting breast cancer cell proliferation and invasion (McAllister et al., 2010). The degree to which CBD elicits these anti-cancer effects would as well depend on the bioactivity of the CBD.

The bioactivity testing procedure used in this experiment, as described in Cushing et al. (2018), consisted of a monoclonal antibody test whose validity was based on the CB_2 affinity of CBD samples. It is as of yet unclear whether the CBD bioactivity test predicts the calcification reduction effects of non-CB_2 targets, such as GPR55 (Lauckner, Jensen, Chen, Lu, Hille, & Mackie, 2008). We expect that bioactivity generalizes to effects that are mediated through non-CB2 pathways. If so, research that utilized low bioactivity CBD to explore its pro-calcific effects on pathways such as GPR55 may have produced erroneous results. It is imperative that CBD samples be tested for bioactivity prior to clinical research.

Method:

All chemicals and solutions were obtained from Sigma- Aldrich (St. Louis, MO). All cell cultures were obtained from Creative Bioarray, Shirley, NY. CBD bioactivity was measured using practices described in Cushing, Kristipati, Shastri, and Joseph (2018).

VIC isolation and culture

VICs were isolated from porcine aortic valve leaflets (Hormel, Austin, MN) by collagenase digestion and subsequently cultured in growth medium (15% FBS, 2 mML-glutamine, 100 U/ml penicillin, and 100 g/ml streptomycin in medium 199) at 37°C, 5% CO2 for two to four passages. VICs used in all experiments were seeded at a density of 50,000 cells/cm^2 onto 24-well or 96-well plates. During the experiments, the VICs were cultured in low-serum medium (1% FBS, 100 U/ml penicillin, 100 g/ml streptomycin, 2 mM L-glutamine, in medium 199), and the medium was changed each day until the fifth day.

Culture substrate coatings

Tissue culture polystyrene (TCPS) plates (24-well or 96-well) were coated with type I collagen (Coll) (Inamed Biomaterials, Fremont, CA; 2 g/cm2), fibronectin (FN, 5 g/cm2), fibrin (FB, 1.5 g/cm2), or left untreated (TCPS). For the FB coating, plates were first incubated overnight at 4°C in fibrinogen (1 mg/ml), followed by three washes with 0.05% Tween 20 in phosphate- buffered saline (PBS) and 1 h incubation with thrombin (0.6 mg/ml) at 37°C (12). All coatings were prepared in 50 mM bicarbonate coating

buffer, pH 8.5, and rinsed three times with PBS before cell seeding. The amounts of adsorbed proteins were measured on separate plates using the bicinchoninic acid protein assay (Pierce, Rockford, IL) to verify adsorption of protein coatings.

MEK-1/2 inhibition

VICs exposed to various concentrations and bioactivities of CBD were treated with U-0126 [1,4-diamino- 2,3-dicyano-1,4-bis(2- aminophenylthio) butadiene; Calbiochem, San Diego, CA], PD-98059 (2-amino-3 methoxyflavone; 5 M; Calbiochem), or left untreated as a control to confirm the MAPK specificity of these inhibition experiments. U-0126 specifically inhibits MEK-1/2, thus inhibiting activation of ERK-1/2 (Favata et al., 1998). PD-98059 is an alternate MEK inhibitor. 9 tissue samples were in each treatment group. These were the tissue samples used in subsequent analyses.

Quantification of cell number

At time points of 1, 3, and 5 days, VICs were lysed with radioimmunoprecipitation assay buffer [1% sodium deoxycholate, 0.1% SDS, 1% Triton X-100, 1 mM iodoacetamide, 140 mM NaCl, 10 mM Tris HCl, (pH 8.0)]. The amount of DNA in sample lysates was measured via the Quanti-iT PicoGreen assay (Invitrogen, Carlsbad, CA), according to the manufacturer's instructions.

Migration assay

Migration was assayed via a modified fence method (Mann & West, 2002), wherein VICs were seeded within 2 mm^2 removable silicone wells, grown to confluency, and then allowed to migrate following the detachment of silicone isolators (defined as day 0). Grid-patterned transparencies were attached underneath plates containing VIC cultures to track cell movement over time. Photomicrographs were taken of the leading edge of cell migration under 40 magnification (Olympus IX51) every 24 h for 5 days. Net cell edge displacement was measured by overlaying time course images and then quantifying migration distance (NIH ImageJ) by measuring the advancement of the leading cell edge subtracted from the migration area recorded on day 0 within a single grid space.

Apoptosis assay

To ensure the health of the cell samples used in the calcification experiment, apoptosis was measured using an ELISA-based HT TiterTACS Assay Kit (Trevigen, Gaithersburg, MD), which detects DNA fragmentation. At days 1 and 5, cells were fixed in 3.7% buffered formaldehyde solution for 7 min, washed with PBS, and postfixed in 100% methanol for 20 min. Following manufacturer's instructions, the cells were permeabilized with proteinase K, quenched with 2.5% H2O2 in methanol, and then incubated with the labeling reaction mix (TdT, Biotin-dNTP, unlabeled dNTP) to label breaks in DNA. Streptavidin-HRP and then TACS-Sapphire were added to the wells to detect apoptotic cells; the reaction was stopped with 2 N HCl, and absorbance was read at 450 nm.

RNA isolation

Total RNA was isolated using TRI Reagent (Molecular Research Center, Cincinnati, OH), according to the manufacturer's instructions. VICs were lysed with 200 l TRI Reagent per well at 4°C with 50 protease inhibitor cocktail (BD Biosciences, San Jose, CA). The homogenate was stored at room temperature for 5 min to complete the dissociation of nucleoprotein complexes, at which point 0.15 ml chloroform per 600 l TRI Reagent was added to the homogenate, followed by centrifugation at 13,000 g for 15 min. After centrifugation, RNA was precipitated from the upper aqueous phase by adding 0.3 ml isopropanol per 600 l TRI Reagent to the tubes and then centrifuged at 13,000 g for 8 min. After this centrifugation step, the RNA pellet was washed with 75% ethanol and centrifuged at 8,000 g for 5 min. The RNA pellet was air dried and dissolved in 75l H2O at 60°C for 15 min. RNA samples were stored at 20°C until subsequent use.

Quantitative real-time PCR analysis

Custom primers for various markers of cell contractility and osteogenic activity were obtained from Invitrogen (Carlsbad, CA) and are listed in Table 1. For cDNA construction, 250 ng of original RNA isolated from samples were reverse transcribed using iScript (Bio-Rad Laboratories, Hercules, CA) as per manufacturer's instructions. Samples were processed for real-time PCR analysis by combining 0.5 l of the cDNA construction, 5 M of primers, and SYBR Green SuperMix (Bio-Rad) in a 15-l reaction, as specified in the manufacturer's protocol. For thermo cycling, a standard protocol was used: PCR reactions were run over 40 cycles of denaturing at 95°C for

15 s and annealed at 60°C for 1 min; this was followed by a melting curve analysis for 80 cycles of 55°C 0.5°C/cycle, 10 s per cycle, to further confirm the purity of the final PCR products, with each condition performed in triplicate (iCycler iQ Real-Time PCR Instrument, Bio-Rad). A standard comparative threshold cycle (or CT) method was used to analyze the PCR data. The CT of all samples were first normalized to -actin as an internal control, and then the CT values for experimental samples were further normalized to the negative control (VICs on Coll, which represented a non CBD condition).

Quantification of nodule number and size

After 5 days of culture in the presence or absence of U-0126 or PD-98059, VIC cultures were stained with Alizarin Red S (ARS) to facilitate quantification of calcified nodules, as ARS stains mineralized deposits red. Cultures were fixed with 10% neutral buffered formalin, stored at 4°C overnight, and stained with a 2% solution of ARS in PBS. Positively stained nodules were manually counted under a microscope (Olympus IX51 with Hamamatsu 285 digital camera and Simple PCI digital imaging software; Compix, Imaging Systems, Cranberry Township, PA). Nodule size was measured using ImageJ software (National Institutes of Health; http://rsb.info.nih.gov/ij/), and photomicrographs were captured under 40 and 100 magnifications.

CBD samples and bioactivity testing

CBD samples with bioactivities .20, .30, .50, .60, and .70 were obtained from Randy Kindred, Natural Hemp Solutions. CBD samples with bioactivities .80, .90, and .95 were isolated from ImmunAG, a humulus product of ImmunAG LLP. Following isolation, bioactivity was measured using procedures outlined in Cushing, Kristipati, Shastri, and Joseph (2018).

References:

Ahrens, J., Demir, R., Leuwer, M., De La Roche, J., Krampfl, K., Foadi, N., ... & Haeseler, G. (2009). The nonpsychotropic cannabinoid cannabidiol modulates and directly activates alpha-1 and alpha-1-Beta glycine receptor function. *Pharmacology*, *83*(4), 217-222. https://doi.org/10.1159/000201556

Bisogno, T., Hanuš, L., De Petrocellis, L., Tchilibon, S., Ponde, D. E., Brandi, I., ... & Di Marzo, V. (2001). Molecular targets for cannabidiol and its synthetic analogues: effect on vanilloid VR1 receptors and on the cellular uptake and enzymatic hydrolysis of anandamide. *British journal of pharmacology*, *134*(4), 845-852. https://doi.org/10.1038/sj.bjp.0704327

Butcher, J. T., Simmons, C. A., & Warnock, J. N. (2008). Mechanobiology of the aortic heart valve. *Journal of Heart Valve Disease*, *17*(1), 62. https://doi.org/10.1007/978-1-4939-5617-3_12

Costa, B., Giagnoni, G., Franke, C., Trovato, A. E., & Colleoni, M. (2004). Vanilloid TRPV1 receptor mediates the antihyperalgesic effect of the nonpsychoactive cannabinoid, cannabidiol, in a rat model of acute inflammation. *British journal of pharmacology*, *143*(2), 247-250. https://doi.org/10.1038/sj.bjp.0705920

Cushing, D., Kristipati, S., Shastri, R., & Joseph, B. (2018). Measuring the bioactivity of phytocannabinoid cannabidiol from cannabis sources, and a novel non-cannabis source. *Journal of Medical Phyto Research*, *10*. https://doi.org/10.31013/2002b

De Petrocellis, L., Ligresti, A., Moriello, A. S., Allarà, M., Bisogno, T., Petrosino, S., ... & Di Marzo, V. (2011). Effects of cannabinoids and cannabinoid-enriched Cannabis extracts on TRP channels and endocannabinoid metabolic enzymes. *British journal of pharmacology*, *163*(7), 1479-1494. https://doi.org/10.1111/j.1476-5381.2010.01166.x

de Simone, G., Izzo, R., Chinali, M., De Marco, M., Casalnuovo, G., Rozza, F., ... & De Luca, N. (2010). Does information on systolic and diastolic function improve prediction of a cardiovascular event by left ventricular hypertrophy in arterial hypertension?. *Hypertension*, *56*(1), 99-104. https://doi.org/10.1161/hypertensionaha.110.150128

Farrar, E. J., Pramil, V., Richards, J. M., Mosher, C. Z., & Butcher, J. T. (2016). Valve interstitial cell tensional homeostasis directs calcification and extracellular matrix remodeling processes via RhoA signaling. *Biomaterials*, *105*, 25-37. https://doi.org/10.1016/j.biomaterials.2016.07.034

Favata, M. F., Horiuchi, K. Y., Manos, E. J., Daulerio, A. J., Stradley, D. A., Feeser, W. S., ... & Copeland,

R. A. (1998). Identification of a novel inhibitor of mitogen-activated protein kinase kinase. *Journal of Biological Chemistry*, *273*(29), 18623-18632. https://doi.org/10.1074/jbc.273.29.18623

French, J. A., Koepp, M., Naegelin, Y., Vigevano, F., Auvin, S., Rho, J. M., ... & Dichter, M. A. (2017). Clinical studies and anti-inflammatory mechanisms of treatments. *Epilepsia*, *58*, 69-82. https://doi.org/10.1111/epi.13779

Gerdts, E., Rossebø, A. B., Pedersen, T. R., Cioffi, G., Lønnebakken, M. T., Cramariuc, D., ... & Devereux, R. B. (2015). Relation of left ventricular mass to prognosis in initially asymptomatic mild to moderate aortic valve stenosis. *Circulation: Cardiovascular Imaging*, *8*(11), e003644. https://doi.org/10.1161/circimaging.115.003644

Gu, X., & Masters, K. S. (2009). Role of the MAPK/ERK pathway in valvular interstitial cell calcification. *American Journal of Physiology-Heart and Circulatory Physiology*, *296*(6), H1748-H1757. https://doi.org/10.1152/ajpheart.00099.2009

Herrera, B., Carracedo, A., Diez-Zaera, M., Guzmán, M., & Velasco, G. (2005). p38 MAPK is involved in CB2 receptor-induced apoptosis of human leukaemia cells. *FEBS letters*, *579*(22), 5084-5088. https://doi.org/10.1016/j.febslet.2005.08.021

Hjortnaes, J., Shapero, K., Goettsch, C., Hutcheson, J. D., Keegan, J., Kluin, J., ... & Aikawa, E. (2015). Valvular interstitial cells suppress calcification of valvular endothelial cells. *Atherosclerosis*, *242*(1), 251-260. https://doi.org/10.1016/j.atherosclerosis.2015.07.008

Huang, D., Ding, Y., Luo, W. M., Bender, S., Qian, C. N., Kort, E., ... & Teh, B. T. (2008). Inhibition of MAPK kinase signaling pathways suppressed renal cell carcinoma growth and angiogenesis in vivo. *Cancer research*, *68*(1), 81-88. https://doi.org/10.1158/0008-5472.can-07-5311

Idris, A. I., Sophocleous, A., Landao-Bassonga, E., van't Hof, R. J., & Ralston, S. H. (2008). Regulation of bone mass, osteoclast function, and ovariectomy-induced bone loss by the type 2 cannabinoid receptor. *Endocrinology*, *149*(11), 5619-5626. https://doi.org/10.1210/en.2008-0150

Idris, A. I., van't Hof, R. J., Greig, I. R., Ridge, S. A., Baker, D., Ross, R. A., & Ralston, S. H. (2005). Regulation of bone mass, bone loss and osteoclast activity by cannabinoid receptors. *Nature medicine*, *11*(7), 774. https://doi.org/10.1038/nm1255

Kaschina, E. (2016). Cannabinoid CB1/CB2 Receptors in the Heart: Expression, Regulation, and Function. In *Cannabinoids in Health and Disease*. InTech. https://doi.org/10.5772/62822

Lauckner, J. E., Jensen, J. B., Chen, H. Y., Lu, H. C., Hille, B., & Mackie, K. (2008). GPR55 is a cannabinoid receptor that increases intracellular calcium and inhibits M current. *Proceedings of the National Academy of Sciences*, *105*(7), 2699-2704. https://doi.org/10.1073/pnas.0711278105

Lewis, T. S., Shapiro, P. S., & Ahn, N. G. (1998). Signal transduction through MAP kinase cascades. In *Advances in cancer research* (Vol. 74, pp. 49-139). Academic Press. https://doi.org/10.1016/s0065-230x(08)60765-4

Ligresti, A., De Petrocellis, L., & Di Marzo, V. (2016). From phytocannabinoids to cannabinoid receptors and endocannabinoids: pleiotropic physiological and pathological roles through complex pharmacology. Physiological reviews, 96(4), 1593- 1659. https://doi.org/10.1152/physrev.00002.2016

Mann, B. K., & West, J. L. (2002). Cell adhesion peptides alter smooth muscle cell adhesion, proliferation, migration, and matrix protein synthesis on modified surfaces and in polymer scaffolds. *Journal of biomedical materials research*, *60*(1), 86-93. https://doi.org/10.1002/jbm.10042

Michel, E. J. S., & Dipchand, A. I. (2017). Valvular Stenosis and Heart Failure. *Heart Failure in the Child and Young Adult: From Bench to Bedside*, 307. https://doi.org/10.1016/b978-0-12-802393-8.00023-5

Milella, M., Kornblau, S. M., Estrov, Z., Carter, B. Z., Lapillonne, H., Harris, D., ... & Andreeff, M. (2001). Therapeutic targeting of the MEK/MAPK signal transduction module in acute myeloid leukemia. *The Journal of clinical investigation*, *108*(6), 851-859. https://doi.org/10.1172/jci200112807

Mohler III, E. R., Gannon, F., Reynolds, C., Zimmerman, R., Keane, M. G., & Kaplan, F. S. (2001). Bone formation and inflammation in cardiac

valves. *Circulation*, *103*(11), 1522-1528. https://doi.org/10.1161/01.cir.103.11.1522

Mukhopadhyay, P., Rajesh, M., Pan, H., Patel, V., Mukhopadhyay, B., Bátkai, S., ... & Pacher, P. (2010). Cannabinoid-2 receptor limits inflammation, oxidative/nitrosative stress, and cell death in nephropathy. *Free Radical Biology and Medicine*, *48*(3), 457-467. https://doi.org/10.1016/j.freeradbiomed.2009.11.022

Naito, Y., Tsujino, T., Akahori, H., Ohyanagi, M., Mitsuno, M., Miyamoto, Y., & Masuyama, T. (2010). Augmented cannabinoid receptors expression in human aortic valve stenosis. *International journal of cardiology*, *145*(3), 535-537. https://doi.org/10.1016/j.ijcard.2010.04.067

Ofek, O., Karsak, M., Leclerc, N., Fogel, M., Frenkel, B., Wright, K., ... & Mechoulam, R. (2006). Peripheral cannabinoid receptor, CB2, regulates bone mass. *Proceedings of the National Academy of Sciences*, *103*(3), 696-701. https://doi.org/10.1073/pnas.0504187103

Pazos, M. R., Mohammed, N., Lafuente, H., Santos, M., Martínez-Pinilla, E., Moreno, E., ... & Hillard, C. J. (2013). Mechanisms of cannabidiol neuroprotection in hypoxic–ischemic newborn pigs: Role of 5HT1A and CB2 receptors. *Neuropharmacology*, *71*, 282-291. https://doi.org/10.1016/j.neuropharm.2013.03.027

Ross, R. A. (2009). The enigmatic pharmacology of GPR55. *Trends in pharmacological sciences*, *30*(3), 156-163. https://doi.org/10.1016/j.tips.2008.12.004

Ross, H. R., Napier, I., & Connor, M. (2008). Inhibition of recombinant human T-type calcium channels by Δ9-tetrahydrocannabinol and cannabidiol. *Journal of Biological Chemistry*, *283*(23), 16124-16134. https://doi.org/10.1074/jbc.m707104200

Roy, J., Kazi, M., Hedin, U., & Thyberg, J. (2001). Phenotypic modulation of arterial smooth muscle cells is associated with prolonged activation of ERK1/2. *Differentiation*, *67*(1-2), 50-58. https://doi.org/10.1046/j.1432-0436.2001.067001050.x

Salasznyk, R. M., Klees, R. F., Hughlock, M. K., & Plopper, G. E. (2004). ERK signaling pathways regulate the osteogenic differentiation of human mesenchymal stem cells on collagen I and vitronectin. *Cell communication & adhesion*, *11*(5-6), 137-153. https://doi.org/10.1080/15419060500242836

Steffens, S., Veillard, N. R., Arnaud, C., Pelli, G., Burger, F., Staub, C., ... & Mach, F. (2005). Low dose oral cannabinoid therapy reduces progression of atherosclerosis in mice. *Nature*, *434*(7034), 782-786. https://doi.org/10.1038/nature03389

Taylor, P. M., Batten, P., Brand, N. J., Thomas, P. S., & Yacoub, M. H. (2003). The cardiac valve interstitial cell. *The international journal of biochemistry & cell biology*, *35*(2), 113-118. https://doi.org/10.1016/s1357-2725(02)00100-0

Thomas, A., Baillie, G. L., Phillips, A. M., Razdan, R. K., Ross, R. A., & Pertwee, R. G. (2007). Cannabidiol displays unexpectedly high potency as an antagonist of CB1 and CB2 receptor agonists in vitro. *British journal of pharmacology*, *150*(5), 613-623. https://doi.org/10.1038/sj.bjp.0707133

Qin, N., Neeper, M. P., Liu, Y., Hutchinson, T. L., Lubin, M. L., & Flores, C. M. (2008). TRPV2 is activated by cannabidiol and mediates CGRP release in cultured rat dorsal root ganglion neurons. *Journal of Neuroscience*, *28*(24), 6231-6238. https://doi.org/10.1523/jneurosci.0504-08.2008

Ivanov, V. N., Wu, J., & Hei, T. K. (2017). Regulation of human glioblastoma cell death by combined treatment of cannabidiol, γ-radiation and small molecule inhibitors of cell signaling pathways. *Oncotarget*, *8*(43), 74068. https://doi.org/10.18632/oncotarget.18240

Wagner, E. F., & Nebreda, Á. R. (2009). Signal integration by JNK and p38 MAPK pathways in cancer development. *Nature Reviews Cancer*, *9*(8), 537. https://doi.org/10.1038/nrc2694

Whyte, L. S., Ryberg, E., Sims, N. A., Ridge, S. A., Mackie, K., Greasley, P. J., ... & Rogers, M. J. (2009). The putative cannabinoid receptor GPR55 affects osteoclast function in vitro and bone mass in vivo. *Proceedings of the National Academy of Sciences*, *106*(38), 16511-16516. https://doi.org/10.1073/pnas.0902743106

Appendix: All VIC calcification reduction data.

Concentration	Sample ID	Bioactivity .20	.30	.50	.60	.70	.80	.90	.95
5mg	1548	4.2	5.5	10.4	8.7	8.6	13.0	18.5	21.9
5mg	1730	4.8	5.7	8.2	8.2	13.6	13.8	19.3	19.2
5mg	1194	4.7	5.9	9.1	7.4	11.6	16.4	17.8	21.4
5mg	1785	5.5	6.4	7.8	8.1	11.1	13.1	21.0	21.2
5mg	1772	6.9	6.9	7.5	7.0	10.7	15.1	18.0	18.9
5mg	1169	3.8	6.1	7.1	9.1	10.5	15.3	17.9	19.7
5mg	1245	4.1	5.6	7.8	7.3	9.9	14.2	16.0	19.8
5mg	1496	4.1	6.4	7.9	8.8	10.3	13.8	14.6	19.4
5mg	1381	6.1	6.7	7.6	5.3	10.7	13.9	18.1	20.5
5mg	1380	4.4	5.5	8.2	6.3	10.7	13.6	18.6	16.7
5mg	1230	6.3	5.3	6.2	7.4	7.3	16.0	17.2	21.7
5mg	1655	5.0	6.1	10.0	7.2	11.2	15.0	17.7	18.8
5mg	1175	5.4	6.2	7.4	7.7	11.6	11.3	17.7	19.8
5mg	1617	6.4	6.3	7.8	7.4	8.0	14.0	18.5	17.6
5mg	1042	6.4	6.3	7.5	7.6	9.5	14.1	19.1	18.5
5mg	1640	5.3	6.0	8.3	6.2	9.1	14.6	16.5	18.8
5mg	1082	4.3	5.3	8.1	7.5	11.0	14.6	19.0	16.5
5mg	1743	5.2	7.3	7.9	8.1	9.7	15.9	19.2	18.5
5mg	1278	5.3	6.5	8.2	8.9	10.1	15.4	17.8	22.1
5mg	1134	4.3	6.4	8.1	7.5	9.7	14.6	18.7	20.4
5mg	1452	5.4	5.2	7.8	7.6	9.5	16.5	17.5	16.6
5mg	1696	5.5	6.4	7.7	7.8	8.8	16.6	19.5	19.7
5mg	1765	6.0	5.8	8.7	7.5	9.6	13.3	18.1	18.7
5mg	1032	5.7	6.3	7.8	6.8	10.5	12.4	17.8	21.1
5mg	1850	4.5	6.6	7.7	7.3	9.5	13.1	18.7	21.9
5mg	2018	4.6	6.5	6.8	8.8	10.3	14.7	17.0	15.4
5mg	1205	5.4	7.0	8.2	8.5	8.5	12.3	17.8	19.6
10mg	1548	3.7	6.6	8.8	12.7	15.0	17.5	23.1	32.5
10mg	1730	4.6	6.4	11.2	11.6	14.4	19.1	20.5	18.5
10mg	1194	4.5	6.5	10.0	11.4	13.5	22.8	20.9	24.2
10mg	1785	5.9	6.5	9.3	11.9	12.8	18.9	26.2	27.9
10mg	1772	4.7	5.3	10.2	10.6	16.0	21.7	24.5	26.8
10mg	1169	4.7	5.3	9.1	12.1	15.7	16.2	29.6	24.0
10mg	1245	4.9	5.6	9.1	9.2	13.6	17.1	23.5	20.8
10mg	1496	5.1	7.1	10.8	14.3	10.2	18.8	28.3	31.0
10mg	1381	4.9	5.9	9.2	12.7	12.4	16.4	22.4	27.9
10mg	1380	3.9	6.6	9.2	11.2	15.5	19.5	24.7	25.4
10mg	1230	5.4	7.0	10.9	11.6	15.1	22.5	23.2	25.1
10mg	1655	5.9	5.9	9.5	10.8	15.6	22.9	28.6	27.0
10mg	1175	4.5	6.7	9.9	11.4	13.3	22.0	25.4	22.6
10mg	1617	6.2	6.1	10.6	11.4	14.4	20.9	23.8	28.1
10mg	1042	4.5	6.6	11.4	11.5	15.3	21.9	21.5	27.1
10mg	1640	4.6	6.8	10.6	11.9	14.0	18.6	26.9	22.3
10mg	1082	5.0	5.2	8.6	10.8	17.2	22.7	23.1	28.7
10mg	1743	3.7	4.9	7.7	13.1	13.5	24.1	24.5	24.3
10mg	1278	5.2	5.3	11.7	14.0	16.9	20.2	24.4	23.5
10mg	1134	5.2	6.7	10.0	11.9	15.0	16.0	24.0	25.7
10mg	1452	5.2	6.2	9.1	11.4	14.5	15.9	24.4	26.3
10mg	1696	4.8	6.5	9.2	10.4	13.5	24.6	29.6	24.8
10mg	1765	5.1	6.1	9.1	12.6	13.9	20.7	25.6	27.2
10mg	1032	5.2	7.5	10.2	12.7	12.6	20.3	26.0	27.4
10mg	1850	5.8	6.2	10.8	12.6	13.4	19.0	27.0	21.3

10mg	2018	5.0	5.9	8.8	12.3	14.1	20.8	24.0	25.6
10mg	1205	5.4	7.1	8.8	10.6	15.4	19.8	30.3	24.1
25mg	1548	5.6	5.5	11.9	15.3	16.3	28.5	31.6	34.9
25mg	1730	5.9	7.1	10.3	13.1	14.8	27.7	34.4	27.7
25mg	1194	6.8	6.9	11.8	14.6	16.3	22.4	31.6	34.0
25mg	1785	5.7	6.6	10.7	12.7	14.7	22.7	28.3	29.2
25mg	1772	6.3	6.7	11.1	13.5	18.4	20.2	31.7	34.4
25mg	1169	5.2	6.1	10.5	14.2	18.6	27.2	31.5	30.3
25mg	1245	6.0	7.2	10.4	13.1	17.0	29.9	25.5	34.8
25mg	1496	5.5	8.1	11.0	13.5	17.0	25.9	30.1	31.6
25mg	1381	5.8	6.1	11.5	13.8	15.0	23.3	35.1	31.4
25mg	1380	6.3	4.9	10.0	14.6	15.5	25.0	29.1	42.4
25mg	1230	5.6	7.6	10.2	13.1	18.4	27.7	33.1	29.7
25mg	1655	7.1	4.9	12.1	13.4	15.8	28.2	30.8	42.6
25mg	1175	6.9	6.8	10.9	14.3	15.6	23.9	29.1	32.3
25mg	1617	5.7	4.6	9.8	12.8	18.0	24.6	28.4	35.6
25mg	1042	6.1	7.0	11.9	10.5	17.8	30.3	23.5	34.1
25mg	1640	5.7	5.0	11.1	14.0	16.3	25.5	32.9	31.0
25mg	1082	6.4	6.6	11.4	13.3	17.9	24.6	27.9	30.4
25mg	1743	6.2	5.6	11.4	14.6	14.3	22.4	26.8	29.7
25mg	1278	5.4	6.9	10.7	13.3	14.6	24.2	33.7	39.3
25mg	1134	6.7	6.4	11.5	15.0	17.9	22.6	27.5	34.3
25mg	1452	6.5	6.9	10.6	14.2	17.6	23.1	27.1	38.9
25mg	1696	4.8	6.2	11.3	14.2	16.9	23.2	35.6	28.6
25mg	1765	6.4	5.6	12.5	14.2	16.6	26.5	29.9	32.2
25mg	1032	6.4	5.4	9.8	13.2	18.3	25.2	30.4	31.9
25mg	1850	6.2	6.3	10.4	13.7	16.7	24.9	31.0	26.5
25mg	2018	6.3	5.3	9.7	14.8	15.0	20.6	33.2	28.6
25mg	1205	6.4	5.9	9.5	14.3	15.6	23.1	33.9	26.3
40mg	1548	3.8	7.9	12.4	21.9	30.0	32.3	40.6	39.6
40mg	1730	5.2	7.8	16.0	18.1	28.2	27.6	34.7	43.0
40mg	1194	5.3	7.6	12.1	20.4	24.6	32.8	42.1	47.9
40mg	1785	4.9	7.8	13.2	20.2	24.7	34.6	44.6	42.6
40mg	1772	5.2	7.5	13.9	17.3	24.8	23.4	37.5	47.7
40mg	1169	4.7	5.8	17.1	18.0	29.7	30.6	39.6	46.8
40mg	1245	4.6	6.6	14.9	19.8	25.7	29.7	38.1	47.1
40mg	1496	4.7	8.0	14.9	21.2	19.9	29.1	39.4	44.8
40mg	1381	4.4	6.0	13.2	17.6	22.1	29.0	38.5	46.7
40mg	1380	6.3	7.7	14.7	16.8	24.3	27.9	42.4	36.5
40mg	1230	5.4	6.9	16.5	19.2	33.0	29.4	41.5	36.7
40mg	1655	5.5	6.2	15.4	18.6	22.6	29.2	43.1	43.0
40mg	1175	3.6	7.3	13.8	20.4	24.9	26.7	36.2	38.5
40mg	1617	4.5	6.9	13.3	19.3	18.9	22.4	42.3	51.1
40mg	1042	5.0	6.7	12.6	21.7	25.9	33.9	43.1	41.6
40mg	1640	4.7	8.1	13.2	17.1	22.5	26.2	42.1	46.1
40mg	1082	5.3	7.7	15.0	19.7	22.8	29.5	38.8	37.9
40mg	1743	6.2	6.8	13.9	20.2	24.3	25.3	36.0	36.9
40mg	1278	5.9	8.1	15.2	17.6	19.8	23.6	40.2	44.1
40mg	1134	5.7	7.0	14.2	21.6	24.4	27.0	39.4	42.1
40mg	1452	5.2	7.2	14.2	19.7	23.9	26.5	40.1	39.2
40mg	1696	6.0	6.8	12.0	17.9	25.3	27.6	39.6	35.8
40mg	1765	6.9	8.0	14.8	17.4	23.2	30.6	41.9	39.6
40mg	1032	5.2	6.6	15.2	20.6	25.5	31.6	33.7	38.9
40mg	1850	5.0	5.1	16.3	18.8	27.4	27.9	42.8	44.1
40mg	2018	6.1	7.0	12.6	18.5	21.4	27.8	43.4	47.6
40mg	1205	4.7	7.3	12.7	19.6	27.2	28.4	40.7	54.5

100mg	1548	6.0	7.9	16.1	23.7	30.2	41.6	51.8	52.5
100mg	1730	6.5	6.9	16.0	19.9	26.8	38.8	51.9	43.0
100mg	1194	5.3	8.4	16.5	21.6	35.6	40.1	49.3	59.8
100mg	1785	5.8	6.9	14.9	21.7	31.6	35.8	47.4	55.6
100mg	1772	6.1	7.4	17.9	20.7	30.5	39.2	53.8	59.0
100mg	1169	5.4	7.3	14.8	21.7	29.7	44.4	47.6	50.7
100mg	1245	6.1	8.1	15.3	22.6	32.2	39.2	49.8	51.4
100mg	1496	5.8	6.7	14.1	21.4	29.4	33.8	53.6	41.9
100mg	1381	6.5	7.7	15.7	22.1	29.3	35.6	51.6	60.4
100mg	1380	6.5	6.7	16.4	20.5	30.4	39.6	45.2	62.0
100mg	1230	6.8	7.6	16.4	18.3	29.6	38.2	44.9	66.1
100mg	1655	6.5	6.9	15.0	22.5	31.9	36.3	50.3	59.6
100mg	1175	5.7	6.5	15.9	22.5	31.1	36.1	44.4	63.2
100mg	1617	5.2	7.8	18.1	21.8	31.1	37.1	45.0	51.5
100mg	1042	6.2	6.7	16.5	21.6	27.7	35.0	53.9	57.0
100mg	1640	6.6	6.0	17.1	20.5	30.4	39.7	38.3	64.7
100mg	1082	5.5	6.5	15.5	21.3	31.5	31.7	54.7	58.4
100mg	1743	6.4	7.1	16.7	20.7	29.6	41.8	46.6	56.7
100mg	1278	7.4	7.4	15.8	21.8	32.0	39.5	37.6	41.9
100mg	1134	5.9	7.5	14.3	19.3	31.5	39.7	46.0	51.9
100mg	1452	5.8	7.3	17.3	22.8	33.1	37.2	51.5	43.6
100mg	1696	7.5	8.4	15.7	22.0	35.0	38.5	51.8	56.6
100mg	1765	5.8	7.6	15.4	22.4	32.2	35.9	47.4	56.3
100mg	1032	6.5	6.2	17.3	22.4	27.9	36.5	47.9	59.3
100mg	1850	5.7	6.7	17.4	23.3	31.5	39.9	47.5	52.0
100mg	2018	5.6	6.6	15.5	20.3	31.7	34.8	50.3	53.6
100mg	1205	5.6	7.6	17.2	22.3	25.8	33.1	50.0	56.4

Citation: Cushing, D., Goakar, D., Joseph, B. (2018). Higher bioactivity cannabidiol in greater concentration more greatly reduces valvular interstitial cell calcification. *Journal of Medical Phyto Research, 2*(2), 14-26. https://doi.org/10.31013/2001f

Recieved: August 25, 2018

Accepted: September 7, 2018

Published: September 26, 2018